Available online at www.sciencedirect.com
SCIENCE DIRECT
Catalysis Today 115 (2006) 235–241
CATALYSIS TODAY
www.elsevier.com/locate/cattod

A comparative study on catalytic performances of chromium incorporated and supported mesoporous MSU-*x* catalysts for the oxidehydrogenation of ethane to ethylene with carbon dioxide

Licheng Liu [a,b], Huiquan Li [a,*], Yi Zhang [a]

[a] *Institute of Process Engineering, Chinese Academy of Sciences, P.O. Box 353, Beijing 100080, PR China*
[b] *Graduate School of Chinese Academy of Sciences, Beijing 100049, PR China*

Available online 31 March 2006

Abstract

Two kinds of Cr-based mesoporous materials, Cr incorporated and supported silicate MSU-1, were synthesized at room temperature and characterized with XRD, N_2 adsorption–desorption, FT-IR, DR UV–vis and H_2-TPR techniques. Both Cr-based catalysts exhibited similar mesoporous channels and textural properties. The catalytic performances of two catalysts for the oxidative dehydrogenation of ethane to ethylene with CO_2 were investigated. They both showed high activities, providing 58.0 and 68.1% ethane conversion and 53.4 and 55.6% ethylene yield at 700 °C, respectively. The catalysts were prone to deactivate in the reaction but could be partially regenerated by oxygen. Cr species formed in high oxidation state were reduced during the reaction. It was proposed that these high-valent Cr species were responsible for the high activities of catalysts.

Keywords: Mesoporous material; Catalyst; Oxidative dehydrogenation; Carbon dioxide; Ethane

1. Introduction

The utilization of carbon dioxide (CO_2), as one of the most important green house gases, has been paid worldwide attention. In the past decades, most efforts have concentrated on the utilization of CO_2 as a source of carbon. Just recently, it is realized that CO_2 might also be utilized as a nontraditional oxygen source or oxidant [1,2]. CO_2 has been found to enhance the dehydrogenation of ethane [3,4] and propane [5,6]. The use of CO_2 as an oxidant for the oxidative dehydrogenation (ODH) of lower alkanes into corresponding alkenes is becoming important because of the growing requirement for alkenes. The catalytic oxidehydrogenation of lower alkanes with CO_2 can overcome high energy consumption derived from the highly endothermic thermal pyrolysis and avoid deep oxidation occurred in those process using oxygen as oxidant. Chromium-based catalysts were high active and selective since silica- and alumina-supported chromium oxides have been industrially used for the productions of lower alkenes such as ethylene, propene and isobutene through the dehydrogenation of the corresponding alkanes [2].

The promoting effect of CO_2 in the ODH of ethane was first reported by Wang et al. [7]. Nakagawa et al. [8] studied the dehydrogenation of ethane by CO_2 over several oxides and reported that gallium oxide is an effective catalyst for this reaction, resulting a ethylene yield of 18.6% with a selectivity of 94.5% at 650 °C. Wang et al. [9] investigated the effect of support such as Al_2O_3, SiO_2, TiO_2 and ZrO_2 on the catalytic ODH of ethane to ethylene by CO_2 over several supported Cr_2O_3 catalysts. 8 wt% Cr_2O_3/SiO_2 catalysts could produce a 61% ethane conversion and 55.5% ethylene yield. The distribution of Cr_2O_3 on the supports and surface chromium species structure, which determined the activity of catalysts, was influenced by the nature of supports. Xu et al. [10] investigated catalytic performance of 5K0.5Ni9Mn7Cr/Si-2 catalyst in detail and 66.9% conversion to ethane and 85.3% selectivity to ethylene were achieved at 800 °C. We have prepared nano-sized composite catalyst Cr_2O_3/MgO, which produced 61.54% conversion to ethane and 94.79% selectivity to ethylene in the ODH of ethane with CO_2 at 700 °C [11].

A new family of mesoporous molecular sieves, which possess uniform mesoporous channels with controllable pore

* Corresponding author. Tel.: +86 10 82610244; fax: +86 10 62561822.
E-mail address: hqli@home.ipe.ac.cn (H. Li).

0920-5861/$ – see front matter
doi:10.1016/j.cattod.2006.02.040

sizes as well as a high surface area, was discovered in the 1990s [12–14]. They could be used as a promising catalyst support [15–18]. In all kinds of mesostructure molecular sieves, MSU-*x* was characterized by 3D worm-like holes which favor the diffusion of molecular objects [19,20]. Polyethylene oxides, used as templates in the synthesis of MSU-*x*, are characteristically low-cost, non-toxic and biodegradable. It is well known that the dispersion, the oxidation state and the structural features of supported species may strongly depend on the support. Therefore, studies of chromium species introduced into MSU-*x* would thus be useful in developing Cr-containing catalysts with desirable catalytic activities for ethane dehydrogenation.

In this paper, we investigated the catalytic performance of chromium-based mesoporous molecular sieves for this reaction, including Cr incorporated MSU-1 (Cr-MSU-1) and Cr supported MSU-1 (Cr/MSU-1). Sodium silicate, chromium nitrate and fatty alcohol polyoxyethylene ether ($A(EO)_9$) were used as the source of silicone, metal and mesostructure-directing agent, respectively. MSU-1 and Cr-MSU-1 were prepared at room temperature; Cr/MSU-1 was prepared by wet impregnation method. The catalysts are characterized with XRD, N_2 adsorption–desorption isotherm, FT-IR, DR UV–vis and H_2-TPR techniques. The reactivity and stability tests of the catalysts were performed in a micro-reactor and the composition of the tail gas was analyzed by gas chromatograph on line.

2. Experimental

2.1. Catalyst preparation

Cr-MSU-1: The synthesis proceeded with molar composition SiO_2:0.1$A(EO)_9$:0.05$Cr(NO_3)_3{\cdot}9H_2O$:250H_2O. In a typical synthesis, 2.26 g of $A(EO)_9$ and 0.8 g of $Cr(NO)_3{\cdot}9H_2O$ were dissolved in 40 ml of deionized water at 60 °C, cooled by a mixture of water and ice. The resulting solution was then mixed with another solution prepared by dissolving 9.40 g of $Na_2SiO_3{\cdot}9H_2O$ in 100 ml of deionized water under vigorous stirring. The mixed solution was clear but a precipitate appeared after 40 ml of 1 M HCl solution was added to the mixed solution. The resulting gel was stirred at room temperature moderately for 20 h. After separation by filtration, the solid phase was washed with deionized water and air-dried at 60 °C. The obtained samples were calcined under air with a heating rate of 2 °C/min until 600 °C and held for 4 h.

Cr/MSU-1: MSU-1 was synthesized firstly by above method without the addition of $Cr(NO_3)_3$ and then impregnated with $Cr(NO_3)_3$ solution containing the desired amount of chromium. The obtained sample was dried at 120 °C and calcined at 600 °C for 2 h. The content of Cr was calculated to be 5 wt% Cr_2O_3 in the final catalyst product.

All the catalyst samples were screened to particles of 20–40 mesh before reaction.

2.2. Catalyst characterization

XRD measurements were performed on X'pert Pro MPD X-ray diffractometer from PANalytical with Cu Kα radiation (λ = 0.154187 nm), Generator Settings 40 kV, 30 mA, scanning speed at 0.017° and scanning regions at 0.5–6.0°. N_2 adsorption studies were used to examine the porous properties of each sample. The measurements were carried out on Autosorb series ASIMP apparatus from Quantachrome. Before measurements, the samples were degassed at 200 °C under vacuum for 5 h. Calculation of the specific surface area (BET), the pore volume and the pore size distribution (BJH method) were performed with the software of the apparatus.

FT-IR patterns of samples were obtained on SPECTRUM GX II apparatus from Perkin-Elmer. Two milligram sample and 200 mg KBr were mixed and crushed to a wafer. Diffuse reflectance UV–vis spectroscopic measurements were recorded on a UV2100 spectrometer. The spectra were collected at 200–700 nm referenced to $BaSO_4$.

The actual Cr content in the catalyst was determined by using OPTIMA 5300DV inductively coupled plasma-optical emission spectrometry (ICP-OES) manufactured by Perkin-Elmer. The known weight of Cr-MSU-*x* sample was dissolved in the mixture of hydrofluoric acid (HF) and nitric acid (HNO_3) with the volume proportion as 3:1. The solution obtained after complete dissolution was diluted to required volume. The samples were analyzed to determine Cr content by using most sensitive wavelength of 267.716 nm.

H_2-TPR of the catalysts was performed on CHEMBET3000 chemical adsorption apparatus from Quantachrome by using a mixture of 5 vol% H_2/Ar as reducing gas. A 50 mg sample was heated from room temperature to 800 °C at a heating rate of 16 °C/min after pretreated at 300 °C for 1 h in He gas flow. The reduction signal was recorded by a TCD.

2.3. Catalytic test

The catalytic performance for the oxidative dehydrogenation of ethane with CO_2 was carried out in a fixed-bed quartz tubular reactor with inner diameter of 5.0 mm at 550–700 °C and atmospheric pressure. The gas reactant was constituted of $V(CO_2)/V(C_2H_6)$ equal to 3 (molar ratio) and a total flow rate of 12 ml/min. Catalyst load is 0.2 g. The catalyst was pretreated in CO_2 gas flow during the calefactive process. The products were analyzed on line by a gas chromatograph equipped with a packed column Parapork QS and a thermal conductivity detector (Shimadzu GC 14B). The investigations of stability and regeneration were performed at 700 °C on the same apparatus. The reaction was carried out for 3 h with analyzing products every 20 min. Then reactant gases were switched to air gas flow and the catalyst was regenerated in situ by air at reaction temperature for 3 h. The reaction was again started by replacing the air gas flow with a mixture of ethane and CO_2 for another 1 h after regeneration.

3. Results and discussion

3.1. Textural and structural properties

Fig. 1 shows the XRD patterns of samples prepared, including MSU-1, Cr-MSU-1 and Cr/MSU-1. Like other

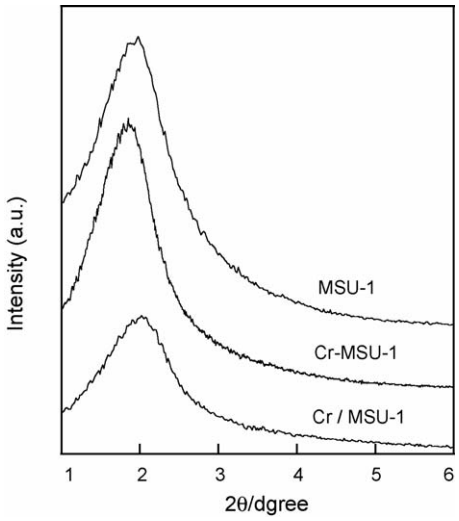

Fig. 1. XRD pattern of MSU-1, Cr-MSU-1 and Cr/MSU-1.

mesoporous MSU-*x* materials, they exhibited only one broad XRD peak at low angle region corresponding to $d_{1\,0\,0}$ reflection [20]. The introduction of Cr atoms had no obvious influence to the meso-structure of MSU-1. The peak intensity of Cr/MSU-1 was lower than those of MSU-1 and Cr-MSU-1. This may arise from the decrease of long-range order of MSU-1 supported with chromium oxides after the second calcination. The peak intensity of MSU-1 was close to Cr-MSU-1 according to the measurements.

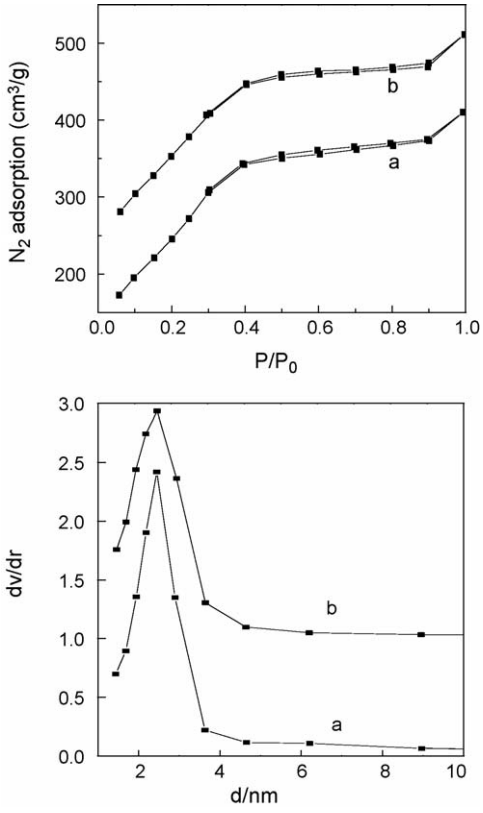

Fig. 2. N_2 adsorption–desorption isotherms and pore size distribution curves of (a) Cr-MSU-1 and (b) Cr/MSU-1.

Table 1
Textural properties and structural parameters of MSU-1, Cr-MSU-1 and Cr/MSU-1

Sample	$d_{1\,0\,0}$ (nm)	Surface area ($m^2\,g^{-1}$)	Pore diameter (nm)	Pore volume ($cm^3\,g^{-1}$)	Wall thickness (nm)
MSU-1	4.51	963.6	2.57	0.62	1.94
Cr-MSU-1	4.75	941.0	2.70	0.63	2.05
Cr/MSU-1	4.25	964.6	2.64	0.64	1.61

The N_2 adsorption–desorption isotherms of Cr-MSU-1 and Cr/MSU-1 were typical of well-defined structural porous framework (Fig. 2), and belong to type IV isotherm indicative of the presence of uniform channels in the super-microporous region as we believed [21]. Zhai et al. [22] prepared mesoporous AlMSU-*x* molecular sieves in the presence of nonionic TX-100 as template. But they considered that the N_2 adsorption isotherm of some calcined samples, which were similar to ours, exhibited type I corresponding to IUPAC's classification. It is the character of porous materials with type I adsorption isotherm that the adsorption achieves saturation at relatively lower pressure and only mono-layer molecular adsorption takes place, which results from either the strong interaction between adsorbent and material or the equal size of adsorbent molecular and pore diameter. The adsorption isotherms of samples we obtained showed an ascending trend with the relative pressure (P/P_0) and achieved saturation at about $P/P_0 = 0.45$. Besides, the pore diameter (2–3 nm) of samples we prepared was larger than N_2 molecular diameter (0.38 nm). So multi-layer molecular adsorption and capillary coacervation should take place, indicating type IV adsorption isotherm. The pore size distribution curves, as presented by the ~0.65 nm (Cr-MSU-1) and ~0.72 nm (Cr/MSU-1) width at half height, showed that both samples contained narrow pore size distribution.

Table 1 summarizes some textural properties and structural parameters of MSU-1, Cr-MSU-1 and Cr/MSU-1 samples from XRD and N_2 adsorption–desorption measurements. Most structural properties of Cr-MSU-1 and Cr/MSU-1 were close to each other except $d_{1\,0\,0}$ spacing (4.75 and 4.25 nm, respectively) and wall thickness (2.05 and 1.61 nm, respectively). This may be attributed to more Cr atoms incorporated into the framework of Cr-MSU-1. The surface area of Cr/MSU-1 (964.6 nm) was very close to that of its predecessor MSU-1 (963.6 nm). The introduction of Cr (by incorporation or impregnation) did not destroy the meso-structure of MSU-1.

3.2. Characterization results of FT-IR and DR UV–vis

FT-IR patterns of mesoporous Cr-MSU-1 and Cr/MSU-1 samples (Fig. 3) showed a broad band in the hydroxyl region between 3700 and 3000 cm^{-1} with maximum in the range 3400–3450 cm^{-1}. This band can be assigned due to surface silanols and adsorbed water molecules [23]. The band at 1630 cm^{-1} can also be assigned to adsorption of physical adsorbed water. Other bands between 1400 and 370 cm^{-1} arise from the framework vibration of molecular sieves, including ν_{as}

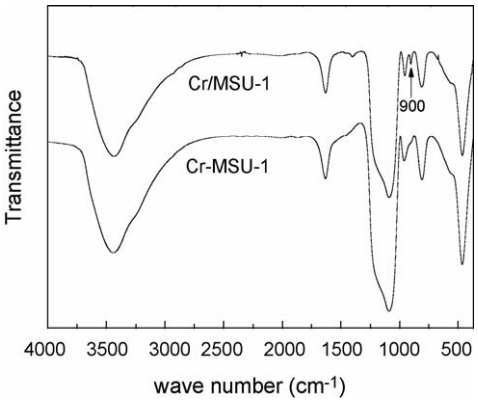

Fig. 3. FT-IR patterns of Cr-MSU-1 and Cr/MSU-1.

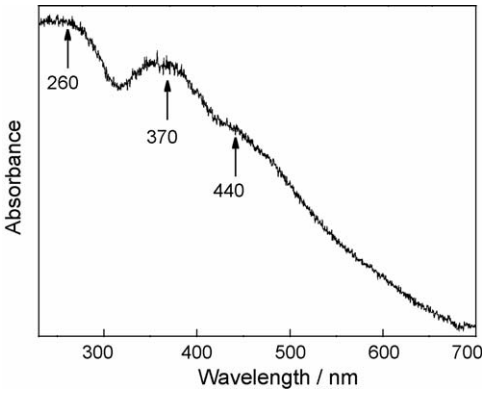

Fig. 4. DR UV–vis spectrum of Cr-MSU-1.

(Si–O–Si), ν_s (Si–O–Si) and δ (Si–O–Si) at 1090, 810 and 460 cm^{-1}, respectively [24]. Interestingly, a weak adsorption band at 900 cm^{-1} appeared for Cr/MSU-1. It may be attributed to the vibration of CrO_4 [25,26]. This band was not observed in the FT-IR spectra of Cr-MSU-1, but the presence of CrO_4 tetrahedra was confirmed by the DR UV–vis spectra of Cr-MSU-1 (Fig. 4). UV bands at 260 and 370 nm and a shoulder around 440 nm are usually assigned to O → Cr(VI) charge transfer absorption bands, indicating that most chromium is Cr(VI) in tetrahedral coordination.

3.3. Catalytic performance

Based on the product distributions, which mainly consist of ethylene, methane, hydrogen and carbon monoxide, and based on other proposed reaction pathways [9,29], we assumed that the following reactions would mostly take place:

$$C_2H_6 \rightarrow C_2H_4 + H_2 \quad (1)$$

$$CO_2 + H_2 \rightarrow H_2O + CO \quad (2)$$

$$CO_2 + C_2H_6 \rightarrow C_2H_4 + H_2O + CO \quad (3)$$

$$C_2H_6 + H_2 \rightarrow 2CH_4 \quad (4)$$

$$C_2H_6 + CO_2 \rightarrow CO + H_2 \quad (5)$$

The ethylene was produced by the direct dehydrogenation of ethane (1) and the oxidehydrogenation of ethane with CO_2 (3), which could also be seen as the summation of reactions (1) and (2). The hydrocracking of ethane (4) and reforming reaction between ethane and CO_2 (5) were the main side reaction. The catalytic performances of Cr-MSU-1 and Cr/MSU-1 varied with reaction temperature are shown in Table 2. Conversions of ethane and CO_2 of two samples both increased with elevation of reaction temperature. The dehydrogenation of ethane with CO_2 exhibited high selectivity to ethylene over Cr-MSU-1 catalyst. It had a bit decrease but still above 90% with elevation of temperature. On the other hand, selectivity to methane increased little by little with temperature, which indicates the elevation of temperature favors hydrocracking of ethane (4).

Table 2
Catalytic performance of mesoporous Cr-MSU-1 and Cr/MSU-1 for oxidative dehydrogenation of ethane with CO_2

Catalyst	T (K)	Conversion (%)		Selectivity (%)			CO/H_2[a]	Yield (%)	TOF (h^{-1})
		C_2H_6	CO_2	C_2H_4	CH_4	CO[b]		C_2H_4	
Cr-MSU-1									
	823	13.4	5.4	96.6	3.4	0	6.4	13.0	32.5
	873	25.1	8.7	95.1	4.9	0	8.0	23.9	61.0
	923	39.8	13.4	94.1	5.8	0.1	8.6	37.5	96.7
	973	58.0	19.1	92.1	7.5	0.4	10.1	53.4	140.9
Cr/MSU-1									
	823	22.6	6.8	70.4	3.9	25.7	11.7	15.9	37.3
	873	30.8	9.3	92.5	7.1	0.4	8.4	28.5	50.9
	923	50.7	22.3	88.4	11.2	0.4	15.1	44.8	83.8
	973	68.1	28.9	81.7	14.2	4.1	17.0	55.6	112.4

Reaction conditions: $V(CO_2)$ = 9 ml/min, $V(C_2H_6)$ = 3 ml/min, catalyst load: 0.2 g, atmospheric.
[a] CO total amounts in the products.
[b] CO produced by ethane reforming.

Similar trends on the variation of conversion and selectivity can be obtained over Cr/MSU-1 catalyst. But lower selectivity to ethylene and higher selectivity to methane were detected. Selectivity to ethylene was only 70.4% at 823 K over Cr/MSU-1 while selectivity to carbon monoxide was 25.7%. It may account for this phenomenon that the reforming reaction of ethane and CO_2 (5) prevails under such condition. However, the production of CO was trivial at other conditions on both catalysts. The CO/H_2 molar ratio increased with temperature because the distinct increase of CO_2 conversion with temperature caused a remarkable increase in the yield of CO.

The actual Cr loading in Cr-MSU-1 and Cr/MSU-1 was determined as 0.86 and 1.20 wt%, respectively, by using ICP-OES. The lower Cr content than that calculated in the synthesis of Cr-MSU-1 is attributed to the high solubility of Cr cations in strong acid solution, resulting in the leaching of Cr during filtration. For Cr/MSU-1, the impregnated and dried sample has been washed once to remove clusters of Cr species on the outer surface and only keep them in the mesoporous channels of MSU-1; this would lead to decrease of Cr loading in the final catalyst. The TOF value was calculated based on the dispersion of Cr on the catalyst surface. Owing to the low Cr loading, Cr dispersions on both Cr-MSU-1 and Cr/MSU-1 were hypothesized to be 100% active [27]. The TOF values (Table 2) on Cr-MSU-1 were larger than that on Cr/MSU-1 in the range of measured temperatures except at 823 K, suggesting that active Cr sites in Cr-MSU-1 was more effective to turn over ethane molecules. It has been a general consensus that chromate and less polychromate (Cr^{6+} and traces of Cr^{5+}) are formed on the surface of supported chromium catalysts at about 1 wt% Cr oxide loading or less [28]. This point is also proved by above FT-IR and DR UV–vis results. In addition, the polychromate:chromate ratio increases with Cr loading [29]. Thus we supposed that monochromate (Cr^{6+}) was the main surface composition of Cr-MSU-1 and Cr/MSU-1 and some polychromate (much more than that on Cr-MSU-1) are formed on the surface of Cr/MSU-1. The higher Cr loading of Cr/MSU-1, which results in the formation of polychromate and more reactive sites provided on catalyst, could well explain that Cr/MSU-1 catalyst exhibited higher activity than Cr-MSU-1 in this reaction under the same conditions [27]. However, the monochromate:polychromate ratios on the surface of catalysts probably influence their selectivity to products. The polychromate and possible small Cr_2O_3 particles formed on Cr/MSU-1 favor some side reactions such as hydrocracking and reforming [30]. Cherian et al. studied the activity of alumina supported chromium oxide for the ODH of propane and found that the activity and selectivity increased with Cr loading under monolayer and decreased for higher loading [31].

3.4. The effect of Cr loading on Cr/MSU-1

It has been generally recognized that the surface chromium species strongly depends on the surface density of chromium oxide [27]. So the effect of Cr loading in Cr/MSU-1 on catalytic performance at reaction temperature 700 °C was investigated. It could be seen from Fig. 5A that 5 wt%Cr/MSU-1 gave the highest activity at this condition. The change of catalytic activity with the variance of Cr_2O_3 loading was related to not only the amount of active sites provided by Cr species but also chromium oxide species [27,28]. When Cr loading was 8 wt%, the diffraction peaks of crystalline α-Cr_2O_3 appeared in the XRD patterns (Fig. 5B). The color of catalysts changes from yellow to green with the growing of Cr content is in accordance with above phenomenon, indicating the formation of Cr(III) at high loadings of Cr. It was similar to the discovery of Hakuli that CrO_x was inclined to form clusters rather than well-dispersed phase with the increase of Cr content on CrO_x/SiO_2 [32]. Yim et al. confirmed that mono, di, tri and tetrachromate species of Cr(VI) and crystalline α-Cr_2O_3 were gradually formed on the surface of Al_2O_3 with increase in the Cr content from 1 to 17 wt% [27]. The formation of crystalline α-Cr_2O_3 correlates well to our result.

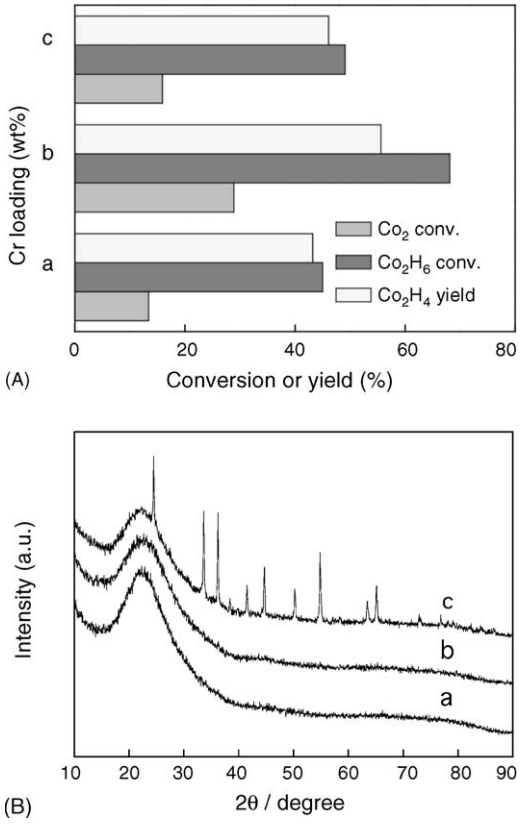

Fig. 5. Catalytic activities (A) and XRD patterns (B) of Cr/MSU-1 with different Cr_2O_3 loading (a) 1 wt%, (b) 5 wt% and (c) 8 wt%.

3.5. Deactivation and regeneration

The catalytic performance over Cr-MSU-1 and Cr/MSU-1 with reaction time and the regeneration by oxygen were investigated, as shown in Fig. 6. Both Cr-MSU-1 and Cr/MSU-1 exhibited higher activities at the beginning of reaction. As the reactions proceeded, conversions of ethane and CO_2 gave a visible drop, suggesting catalysts were deactivated to some degree. For example, conversion of ethane decreased from primal 50.1 to 37.6% over Cr-MSU-1 and 65.0 to 49.2% over Cr/MSU-1, respectively, after reacting for 3 h. However,

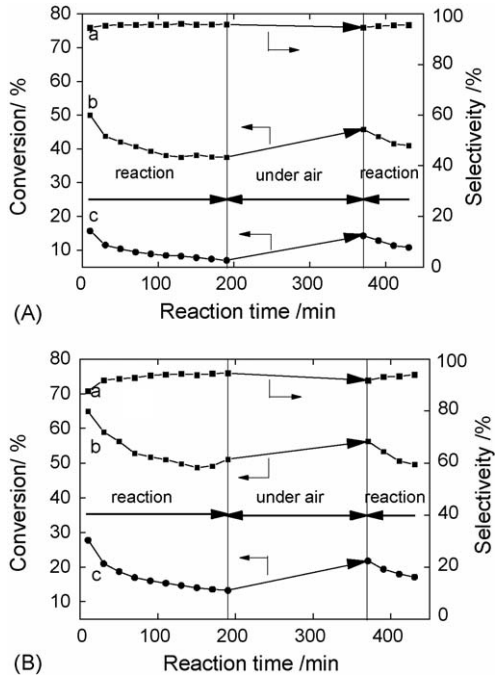

Fig. 6. Reactivity and regeneration with reaction time over (A) Cr-MSU-1 and (B) Cr/MSU-1. (a) Selectivity to ethylene, (b) conversion of ethane and (c) conversion of CO_2.

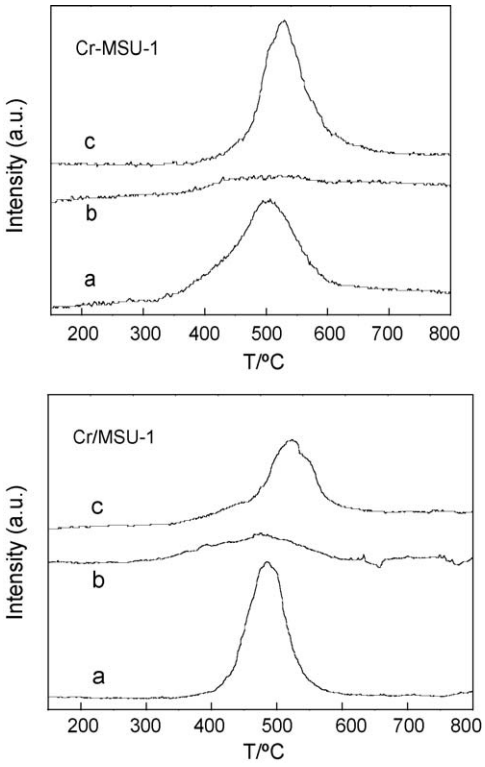

Fig. 7. TPR profiles of Cr-MSU-1 and Cr/MSU-1 catalysts (a) before reaction, (b) after reaction and (c) after regeneration.

selectivity to ethylene gave a slight increase with proceeding reaction, especially over Cr/MSU-1 catalyst. Two kinds of catalysts showed an insufficient but adequately detectable recovery of the activity after treated with air at 700 °C. It is noted that the activity of Cr-MSU-1 got more recovery from the air treatment compared to Cr/MSU-1. Conversion of ethane over Cr-MSU-1 recovered from 37.6 to 45.9%, while that over Cr/MSU-1 recovered from 49.2 to 56.3%. Takehira's investigation revealed that Cr-MCM-41 could be recovered almost completely after reacting for 3 h and treated with O_2 for 5 h whereas Cr/SiO_2 showed an insufficient recovery of the activity after O_2 treatment [2]. These results showed resemblance to ours.

Fig. 7 showed the H_2-TPR profiles of the two catalysts of Cr-MSU-1 and Cr/MSU-1, including before and after reaction and after regeneration. Before the reaction, Cr-MSU-1 sample was reduced from about 350 °C, only one reduction peak was detected between 350 and 600 °C, which could be attributed to the reduction of Cr(VI) or Cr(V) to Cr(III) [2]. Similarly, only one peak was observed between 400 and 600 °C over Cr/MSU-1, which can also be attributed to reduction of Cr(VI) to Cr(III). This is confirmed from FT-IR and UV–vis data showing the presence of Cr(VI) in CrO_4 in two fresh catalysts. After reaction, the reduction peak became smaller, almost disappearing, over both catalysts, suggesting that most Cr(VI) species were reduced to Cr(III) in the reaction. After treated by air at 700 °C for 3 h, Cr(III) species of two catalysts were reoxidized to Cr(VI) (Fig. 7, curves c), the reduction peaks appeared again. Some TPR data, including T_{max} and H_2 consumption (calculated by the peak area for comparative study), are summarized in Table 3. The values in bracket were achieved from Gaussian curve fit of each reduction peak. The peak area in TPR profiles after regeneration were 91% to Cr-MSU-1 and 78% to Cr/MSU-1 of those observed before reaction, suggesting that reoxidation of Cr(III) formed on Cr/MSU-1 was more difficult than that on Cr-MSU-1. It was noteworthy that the T_{max} of both samples moved to high-temperature region after regeneration, compared with that before reaction, although a movement to low-temperature region was observed initially after reaction. This suggested

Table 3
TPR data for Cr-MSU-1 and Cr/MSU-1

	Cr-MSU-1		Cr/MSU-1	
	T_{max} (°C)	H_2 consumption (a.u.)[a]	T_{max} (°C)	H_2 consumption (a.u.)
Before reaction	507 (499)[b]	2300 (1938)	484 (485)	2651 (2358)
After reaction	480	204	474	752
After regeneration	530 (526)	2391 (1770)	523 (516)	2259 (1837)

[a] Calculated by the integral of reduction peak area.
[b] The value in bracket was the result of Gaussian curve fit of each reduction peak.

that the interaction between Cr species and MSU-1 changed in the reaction and regeneration treatment. For fresh catalyst, the T_{max} of Cr/MSU-1 was lower than that of Cr-MSU-1. Thus, a conclusion was probably made that the Cr(VI) species which were prone to be reduced served as the more active sites in catalyst. Combined with the foregoing supposition, these more active Cr(VI) species are related to surface polychromate which are more readily reducible than monochromate [33]. Contrarily, the reduced polychromate are hard to reoxidized to the original form. Therefore, the above phenomenon that the activities of Cr-MSU-1 recover well by the air treatment compared to Cr/MSU-1 could be explained as the incomplete reoxidation of Cr(VI) species (polychromate) on Cr/MSU-1.

From XANES and EXAFS spectra, Takehira et al. [2] concluded that the $Cr(VI)O_4$ tetrahedra were reduced to an aggregated form of the $Cr(III)O_6$ octahedra in Cr-MCM-41 during the reaction of propane and CO_2 and this as the main reason led to the deactivation of Cr-MCM-41. In our experiment, the reduction of Cr(VI) was also observed during reaction. It may play an important role for the deactivation of Cr-MSU-1 and Cr/MSU-1 catalysts. Takahara's investigation [34] showed the partially oxidized Cr_2O_3 supported on SiO_2 catalyst was active for the dehydrogenation of propane and the surface of Cr_2O_3/SiO_2 might be maintained to be partially oxidized in the presence of CO_2. Thus, we believed that Cr(VI) was responsible for the initial high activity of the catalysts, both Cr-MSU-1 and Cr/MSU-1, for the oxidehydrogenation of ethane to ethylene with CO_2. We still investigated the influence of catalyst pretreatment with different gas flow, CO_2 and oxygen. The results suggested that catalyst pretreated with oxygen for 30 min before reaction gave higher conversion of ethane than pretreated with CO_2, for example, 60.0 and 55.9% over Cr-MSU-1. The pretreatment with oxygen could make Cr species in catalyst to be oxidized to higher oxidation state, thus lead to higher activity. This confirmed the conclusion we proposed from another aspect.

4. Conclusion

Mesoporous materials MSU-1 and Cr incorporated Cr-MSU-1 were successfully synthesized with $A(EO)_9$ as template. Chromium supported Cr/MSU-1 prepared by impregnation showed higher activity than Cr-MSU-1 for the oxidative dehydrogenation of ethane to ethylene with carbon dioxide. Cr(VI) acted as active species in the catalysts for initial high activity and the reduction of Cr(VI) to Cr(III) during the reaction resulted in deactivation of catalyst. Both catalysts could be regenerated partially by treated with oxygen.

Acknowledgments

This research was supported by the National Science foundation of China (Grant no. 20436050) and National 863 Program Youth Foundation (Grant no. 2004AA649230).

References

[1] S.B. Wang, Z.H. Zhu, Energy Fuels 18 (2004) 1126.
[2] K. Takehira, Y. Ohishi, T. Shishido, J. Catal. 224 (2004) 404.
[3] N. Mimura, I. Takahara, M. Inaba, M. Okamoto, K. Murata, Catal. Commun. 3 (2002) 257.
[4] S. Wang, K. Murata, T. Hayakawa, S. Hamakawa, K. Suzuki, Appl. Catal. A 196 (2000) 1.
[5] K.L. Fujdala, T.D. Tilley, J. Catal. 218 (2003) 123.
[6] M. Cherian, M.S. Rao, G. Deo, Catal. Today 78 (2003) 397.
[7] D. Wang, M. Xu, C. Shi, J.H. Lunsford, Catal. Lett. 18 (1993) 323.
[8] K. Nakagawa, M. Okamura, N. Ikenaga, T. Suzuki, T. Kobayashi, Chem. Commun. (1998) 1025.
[9] S.B. Wang, K. Murata, T. Hayakawa, S. Hamakawa, K. Suzuki, Appl. Catal. A 196 (2000) 1.
[10] L.Y. Xu, J.X. Liu, H. Yang, Catal. Lett. 62 (1999) 185.
[11] S. Deng, H.Q. Li, Yi Zhang, Chin. J. Catal. 24 (2003) 744.
[12] C.T. Kresge, M.E. Leonowicz, W.J. Roth, J.C. Vartuli, J.S. Beck, Nature 359 (1992) 710.
[13] P.T. Tanev, M. Chibwe, T.J. Pinnavaia, Nature 368 (1994) 321.
[14] D. Zhao, J. Feng, Q. Huo, N. Melosh, G.H. Fredrickson, B.F. Chmelka, G.D. Stucky, Science 279 (1998) 548.
[15] U. Junges, F. Schueth, G. Schmid, Y. Uchida, R. Schloegl, Berl. Bunsen. Phys. Chem. 101 (1997) 1631.
[16] Z. Luan, L. Kevan, J. Phys. Chem. B 101 (1997) 2020.
[17] Z. Zhu, M. Hartmann, E.M. Maes, R.S. Czernuszewicz, L. Kevan, J. Phys. Chem. B 104 (2000) 4690.
[18] S. Kowalak, K. Stawinski, A. Mackowiak, Micropor. Mesopor. Mater. 44–45 (2001) 283.
[19] S.S. Kim, T.R. Pauly, T.J. Pinnavaia, Chem. Commun. (2000) 835.
[20] L. Sierra, J.L. Guth, Micropor. Mesopor. Mater. 27 (1999) 243.
[21] A.B. Stephen, K. Tim, N.B. Milestone, Micropor. Mesopor. Mater. 22 (1998) 419.
[22] S.R. Zhai, W. Wei, D. Wu, Y.H. Sun, Catal. Lett. 89 (2003) 261.
[23] S. Samanta, N.K. Mal, A. Bhaumik, J. Mol. Catal. A 236 (2005) 7.
[24] H.Y. Le, W.M. Hua, Y. Tang, Y.H. Le, Z. Gao, Chem. J. Chin. Univ. 21 (2000) 1101.
[25] S.B. Deng, R.B. Bai, Water Res. 38 (2004) 2424.
[26] M.H. Markus, G.D. John, L.F. John, J. Phys. Chem. A 105 (2001) 6876.
[27] S.D. Yim, I.S. Nam, J. Catal. 221 (2004) 601.
[28] B.M. Weckhuysen, R.A. Schoonheydt, Catal. Today 51 (1999) 223.
[29] B.M. Weckhuysen, R.A. Schoonheydt, J.M. Jehng, I.E. Wachs, S.J. Cho, R. Ryoo, S. Kijlstra, E. Poels, J. Chem. Soc., Faraday Trans. 91 (1995) 3245.
[30] B. Grzybowska, J. Sloczyński, R. Grabowski, L. Keromnes, K. Wcislo, T. Bobińska, Appl. Catal. A 209 (2001) 279.
[31] M. Cherian, M.S. Rao, W.T. Yang, J.M. Jehng, A.M. Hirt, G. Deo, Appl. Catal. A 233 (2002) 21.
[32] A. Hakuli, M.E. Harlin, L.B. Backman, A.O. Krause, J. Catal. 184 (1999) 349.
[33] B.M. Weckhuysen, I.E. Wachs, J. Phys. Chem. 100 (1996) 14437.
[34] I. Takahara, W.C. Chang, N. Mimura, M. Saito, Catal. Today 45 (1998) 55.